



MRS Singapore - ICMAT Symposia Proceedings

7th International conference on materials for advanced technology

Friction stir welded butt joints of AA2024 T3 and AA7075 T6 aluminum alloys

Avinash P^{a,*}, Manikandan M^a, Arivazhagan N^a, Devendranath Ramkumar K^a, Narayanan S^a

^a*School of Mechanical and Building Sciences, VIT University, Vellore, 632014, India*

Abstract

The main objective of this research work is to investigate the feasibility of Friction Stir Welding (FSW) of AA7075 T6 and AA2024 T3 dissimilar aluminum alloys, with thickness ratio of 1.3, and to investigate the mechanical and structural properties of the weld. Since both AA2024 T3 and AA7075 T6 are not weldable by fusion welding processes, FSW process is used to weld both of these dissimilar alloys. Defect-free, tailor weld blanks were produced on the plates of AA7075 T6 and AA 2024 T3 having thickness of 6.5 mm and 5mm respectively. The process parameters employed in this study include the tool rotation and travel speeds. The FSW tool employed in this study was made using AISI H13 tempered steel with square pin profile having pin diameter of 5mm, concavity at pin start of 1mm and pin length of 4.85mm. The welded plates have been characterized for their mechanical and metallurgical properties. The effects of tool rotational speed and the welding speed on the joint performance were discussed.

© 2013 The Authors. Published by Elsevier Ltd.

Selection and/or peer-review under responsibility of the scientific committee of Symposium [Advanced Structural and Functional Materials for Protection] – ICMAT.

Keywords: AA2024; AA7075; FSW; TWB; Dissimilar weld

1. Introduction

Friction Stir Welding (FSW), a relatively newly developed welding technique, has generated significant interest because of the wide range of advantages over the conventional welding techniques. It is a solid-state joining process, where in the materials are welded without reaching their melting temperature, using frictional and adiabatic heat generated by a rotating and traversing cylindrical tool with a profiled pin. The frictional heat generated by the welding tool and the surrounding material causes the softening of the material and allows the tool to be moved along the weld line. Initially, the material is plasticized, and then it is transferred from the leading edge of the tool to trailing edge, leaving a solid-phase bond between the plates. The advantages of this process also encompass better mechanical properties, low residual stress and deformation, and reduced occurrence of defects [1, 2]. The friction stir welded plates, have different regions across the width of the plates: the weld nugget, the thermo-mechanically affected zone (TMAZ) and the heat affected zone (HAZ). The microstructure in the weld nugget is generally found to be very fine and equi-axed, which enhances the ductile property [2, 3]. From the open literatures, it is inferred that the aluminium alloys of 2xxx and 7xxx series are not easily weldable using the conventional techniques. Electrical resistance technique is also used to weld few aluminium alloys. However these techniques require extensive surface preparation and prevention of oxide formation, which is quite difficult to obtain, and

* Corresponding author. Tel.: +91-9047006902; fax: +91-416-224-3092.

E-mail address: avinash.prabakar@gmail.com

thus this limits the use to specific applications [4]. Also, the mechanical properties decrease quite sharply due to the formation of dendritic structure in the weld zone, when welded through conventional fusion techniques [5]. On comparison with the traditional welding processes like the Gas Metal Arc Welding (GMAW), the FSW technique, offers many advantages. FSW is also environment friendly; also the energy required in operating the machinery as well as ancillary equipment, are relatively less when compared with other fusion welding techniques. And, since in FSW, the joining process is accomplished by material flow below the melting temperature, many joint defects caused by joint material melting such as porosity, grain boundary cracks and alloys segregation can be considerably reduced. These process specialties have made FSW very practical for joining dissimilar alloys [6, 7]. The Tailor welded blank of AA2024 and AA7075 finds its application in the automotive sector as well as the aerospace industries, where high strength to weight ratio is the most desirable characteristic property. The FSW technique is also being considered widely as a replacement for fastener, riveted and arc welded joining methods [8, 9]. Furthermore, Tailor Weld Blank (TWB) of different combination of materials by various welding techniques is quite challenging. But with FSW, rapid and high quality welds can be achieved.

This paper discusses the fabrication of TWB of AA2024 and AA7075, having a thickness ratio of 1.3 by FSW technique, as detail studies on dissimilar aluminum alloys having thickness ratio greater than unity are not hitherto reported.

2. Experimental procedure

The base materials employed in this study are 5 mm thick plate of AA2024 and 6.5mm thick plate of AA7075. The aluminium plates were cut into rectangular samples measuring 100 mm x 50 mm. The samples were longitudinally butt-welded using a conventional vertical milling machine with the aid of a specially designed fixture. Also, to compensate for the thickness variation, a support plate of 1.5mm was used as a backing plate (Fig 1 (a)). The macrograph of typical friction stir welded samples is shown in Fig 1 (b).

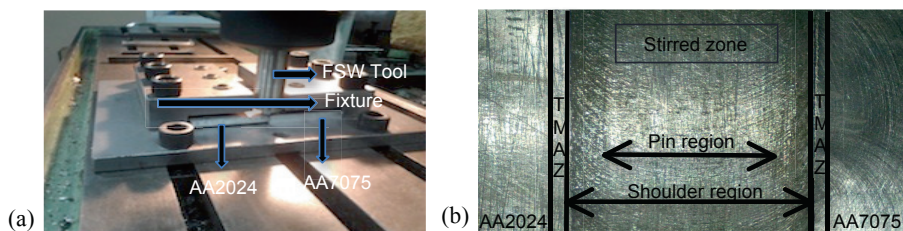


Fig. 1. Illustration of (a) FSW Process carried using conventional milling machine with the aid of specially designed fixture (b) Macrograph of the welded sample.

The welding process was carried out on the samples by keeping AA 7075 T6 as advancing side and AA 2024 T3 on the retreating side. The tool material used in this study was AISI H13 tempered steel with a shoulder of 25 mm diameter along with 5 mm square pin of length 4.8 mm. The process parameters were established based on the existing literatures as well as by trial and error basis. The welds were made with different rotating speeds of 710, 1000 and 1400 rpm and traverse speeds of 80 mm/min and 112 mm/min. Pin offset was maintained to have 1 mm towards the softer material AA2024. For the microstructural characterization, the welded samples were cross-sectioned perpendicularly to the welding direction. The specimens were prepared according to the standard metallographic procedure and were etched using Keller's reagent to reveal the microstructure. Transverse tensile studies were performed at room temperature, on the ASTM E8/8M standard samples using Instron Universal Testing Machine. Hardness measurement was carried out on the composite region of the weldment using Vicker's Micro-hardness tester with 100gf load and dwell time period of 10s, at regular intervals of 0.25 mm. Further, SEM/EDAX and XRD studies were also done to get an in-depth analysis of the formation of various phases on the weldment.

3. Results and discussion

3.1 Metallurgical Characterization:

The TWB of dissimilar AA2024 and AA7075 have been successfully welded using FSW process and no macroscopic defects have been observed in the weldments. The macro-graphic examination revealed the formation of clear semi-circular crown appearance in friction stirred zone as shown in Fig 1(b). This crown appearance majorly depends on the tool shoulder design. Further the formation of such features in FSW is termed as wake effect as reported by Ceschini et al.

[10]. The cavity that was designed between shoulder end and the pin base of the FSW tool has majorly influenced the friction stirred zone by directing the material flow towards the pin. In addition, by providing the cavity, the plasticized materials were confined within the weld line. Hence, this was responsible for the uniform width of the weld region and is represented in Fig 1(b).

The cross sectional macroscopic image of TWB of AA 7075 and AA 2024 and the corresponding micrographs are represented in Fig 2(a-e). It shows the distinct regions of the stirred zone, thermo-mechanically affected zone and heat-affected zone. The stirred region has considerable grain refinement with the precipitates equally distributed after re-precipitation. It is observed that the size of the weld nugget is also larger than the tool pin diameter, which is in accordance with the previous studies [11]. Also, the complete re-crystallization of the grains at the stirred zone is evident from the less deformation. The unmixed region is observed at the top of joints closer to the shoulder region and this could be due to the effect of tool's shoulder and variation in the thickness of base metals (Fig 2(b)). In addition, fine equi-axed grain structures are clearly observed in this zone, which indicates the dynamic recrystallization.

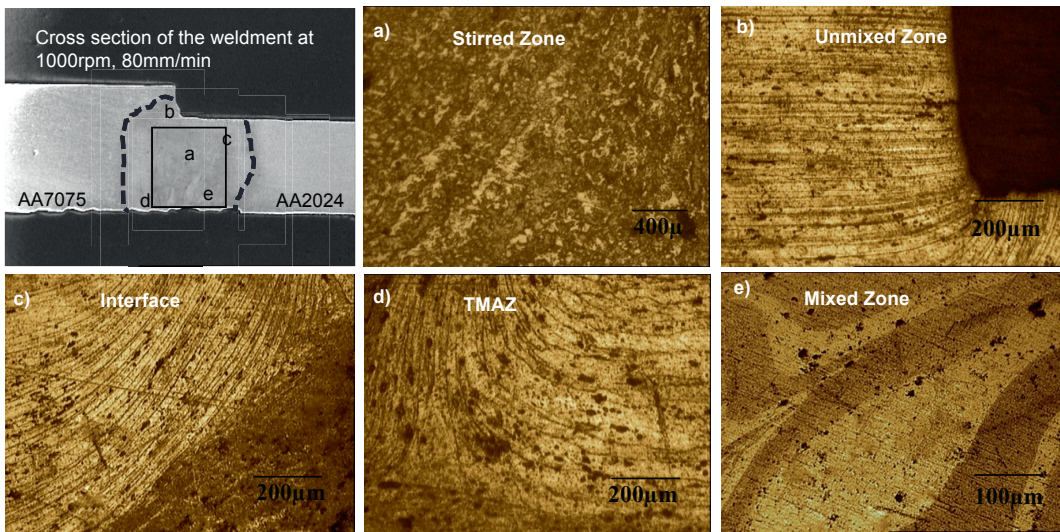


Fig. 2. Microstructure of (a) Stirred Zone (b) Unmixed region showing the thickness variation (c) Interface (d) TMAZ (e) Mixed flow region

The interface region has alternative lamellae of both the base material. Further, at TMAZ, the grains are comparatively large and elongated; this could be due to the decrease in the temperature and degree of the plastic deformation when compared to stirred zone. Also, the high angle grain boundaries have been transformed into low angle grain boundaries, which again confirm the continuous dynamic recrystallization. Jata and Semiatin [12] were the first to propose continuous dynamic recrystallization as operative dynamic nucleation mechanism during FSW. The temperature at TMAZ was relatively lesser than the dissolution temperature during the weld. This accounted for the precipitates to be undissolved during the process, which is evident from the coarsened precipitates at the TMAZ. The etchant revealed AA2024 as darker and AA7075 as lighter in colour; the mixed flow pattern of AA2024 within AA7075 is clearly observed (Fig 2(e)).

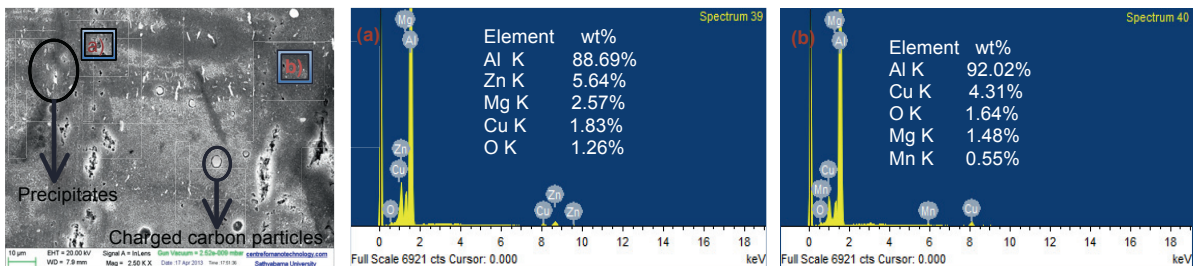


Fig. 3. SEM image of the stirred zone, and the corresponding EDAX analysis at (a) TMAZ and (b) nugget zone.

SEM/EDAX results revealed the random distribution of the precipitates within the weld zone (Fig 3). At the dissolution temperature, precipitates in the weld zone re-precipitated and are arranged in a random fashion during plasticization. EDAX analysis supported the presence of both copper (1.83%) and zinc (5.64%) in the weld nugget, which indicates the efficient stir of both the base materials. Also, the enrichment of zinc is evident, which could be due to the effective stir of AA7075 material, which was kept as the advancing side. The brighter particles could be the charged carbon; since carbon is an insulator, electrons emitted from the SEM could have been trapped within the carbon atom. Presence of carbon is not from either of the base materials; but should have been formed by the reaction of the base materials with etchant that was used to reveal the microstructure.

3.2 Mechanical Characterization

The micro-hardness test result shows the hardness across the weldment. The average micro-hardness value of the TMAZ is relatively higher than that of the stirred zone (Fig 4). This variation could be due to evolution of the precipitates of the precipitate-hardened base materials, which is evident from the micrograph of TMAZ where coarsened precipitates are visible. The lesser hardness in the stirred zone could be due to random distribution of precipitates at the dissolution temperature, which is evident from SEM morphology.

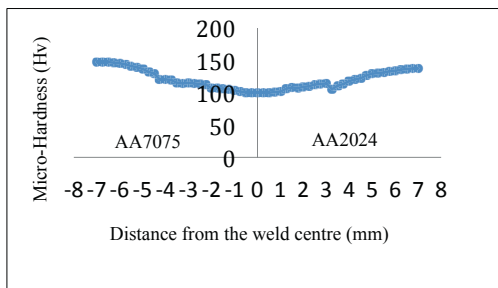


Fig. 4. Micro-hardness profile of the weldment

Table 1. Tensile results of the TWB of dissimilar alloys

Serial No.	Rotational Speed (rpm)	Traverse Speed (mm/min)	Ultimate Tensile Strength (MPa)
1	710	80	148
2	1000	112	204
3	1400	80	261
4	710	112	180
5	1000	80	214
6	1400	112	179

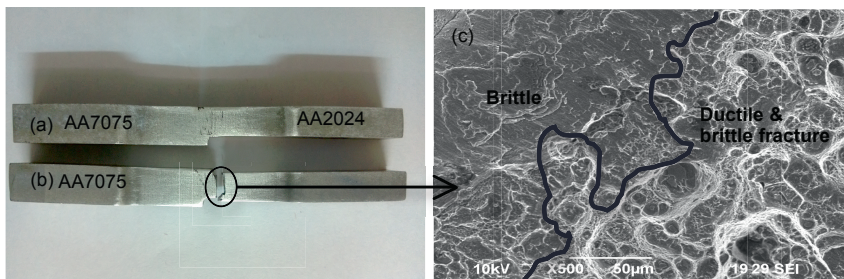


Fig. 5. Tensile studies on dissimilar weldments (a) before fracture (b) after fracture (c) SEM Fractograph.

The tensile studies (table 1) clearly indicate that there is a considerable decrease in the ultimate tensile strength of the welded specimen, when compared with that of the base material. This is mainly due to the higher thickness ratio of 1.3. Previous studies on Laser-TWB, by Chan et al. [13] also confirm that as the thickness ratio increases, there is a significant decrease in most of the mechanical properties. In this scenario, the fracture had occurred in the nugget zone, where there was considerable change in the thickness of both the base materials. From the SEM fractograph (fig 5(b)), it is evident that the fracture was mostly brittle and partly ductile in nature. It also shows the rupture was inter-granular at the stirred zone, with very few micro voids, and is associated with considerable amount of precipitates within the nugget. Also, the failure had started from AA7075 due to the higher stresses that were induced, as it was kept as the advancing side during the welding process.

The results from the X-Ray diffraction (Fig 6) studies indicate the major phases of β Al-Li, $MgAl_2O_4$ and $CrTi_2O_5$ with minor peaks of Al-Cr, Cr-Ti and Al-Fe-Ge, which were formed in the weldment. Further the result shows that most of the phases have been formed with combination of Lithium, which could improve the weldability. In addition, formation of $MgAl_2O_4$ and $CrTi_2O_5$ could be responsible for higher hardness in the weld interface, closer to the TMAZ, which is evident from the micro-hardness analysis (Fig 4).

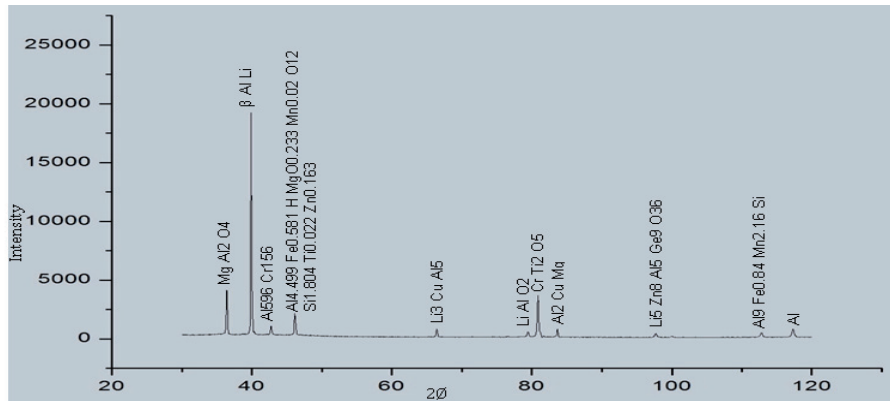


Fig. 6. X-Ray Diffraction results showing the formation of various phases at the stirred zone.

4. Conclusion

- The Tailor welded blank of AA2024 and AA7075, having a thickness ratio of 1.3 have been successfully butt-welded using FS welding technique. Further sound weld has been produced at medium rotational speed (1000 rpm) and lower travel speed (80 mm/min).
- The transformation of the plasticized material from the advancing side to the retreating side is uniform in all the weldments.
- The weld strength is lower as compared to the base metals, which is due to the thickness ratio of the dissimilar welds being greater than unity.
- The partial ductile fracture occurred at the weld nugget, where there was considerable variation in the thickness of the weld samples.
- The grains at the stirred zone are highly refined which is due to the less frictional heat, generated during the process.

References

- [1] Dawes C.J., January, 1995, 'An Introduction to Friction Stir Welding and Its Development, Welding & Met&Fab., p. 12.
- [2] Charit I., Mishra, R.S., Mahoney, M.W., 2002. Multi-sheet structures in 7475 aluminum by friction stir welding in concert with post-weld superplastic forming. *Scripta Materialia* 47, 631–636.
- [3] Rhodes C.G., Mahoney, M.W., Bingel, W.H., Calabrese, M., 2003. Fine-grain evolution in friction-stir processed 7050 aluminum. *Scripta Materialia* 48, 1451–1455.
- [4] Cavaliere, P., Cerri, E., Marzoli, L., Dos Santos, J., Friction stir welding of ceramic particle reinforced aluminium based metal matrix composites, *Applied Composite Materials* 11 (4) (2004) 247–258.
- [5] Su, J.Q., Nelson, T.W., Mishra, R., Mahoney, M., Microstructural investigation of friction stir welded 7050-T651 aluminium, *Acta Materialia* 51 (2003) 713–729.
- [6] Dubourg, L., Merati, A., Jahazi, M., Process optimisation and mechanical properties of friction stir lap welds of 7075-T6 stringers on 2024-T3 skin, *Materials and Design* 31 (2010) 3324–3330
- [7] Vijay Soundararajan, Eswar Yarrapreddy, and Radovan Kovacevic, Investigation of the Friction Stir Lap Welding of Aluminum Alloys AA 5182 and AA 6022, *JMEPEG* (2007) 16:477–484
- [8] John, R., Jata, K.V., Sadananda, K., 2003. Residual stress effects on near threshold fatigue crack growth in friction stir welded aerospace alloys. *International Journal of Fatigue* 25, 939–948.
- [9] Guerra, M., Schmidt, C., McClure, J.C., Murr, L.E., Nunes, A.C., 2003. Flow patterns during friction stir welding, *Materials Characterization* 49, 95–101.
- [10] Ceschini, L., Boromei, I., Minak, G., Morri, A., Tarterini, F., Effect of friction stir welding on microstructure, tensile and fatigue properties of the AA7005/10 vol.%Al₂O_{3p} composite. *Compos Sci Technol* 2007;67:605–15.
- [11] Khodir, S.A., Shibayanagi, T., *Mater. Sci. Eng. B* 148 (2007) 82–87.
- [12] Jata, K.V., Semiatin, S.L., *Scripta Mater.* 43 (2000) 743.
- [13] Chan, L.C., Cheng, C.H., Chan, S.M., Lee, T.C., Chow, C.L., Manuf, J., *Sci. Eng.-Trans. ASME* 127 (2005) 743–751.